PERGAMON International Journal of Engineering Science 37 (1999) 921–943

International Journal of Engineering Science

Regular and chaotic dynamics of a rotational machine with a centrifugal governor

Z.-M. Ge*, H.-S. Yang, H.-H. Chen, H.-K. Chen

Department of Mechanical Engineering, National Chiao Tung University, Hsinchu, Taiwan

Received 10 February 1997; accepted 28 May 1998

Abstract

The dynamic behavior of a rotational machine with centrifugal governor which is subjected to two different forms of external disturbance is studied in this paper. The Lyapunov direct method is applied to obtain conditions of stability of the equilibrium points of the system. A codimension one bifurcation analysis for the autonomous system is carried out near the degenerate point. It is found that a Hopf bifurcation occurs in the system. The incremental harmonic balance (IHB) method combined with the multi-variable Floquet theory has been effectively applied to obtain the steady state responses of the three-dimensional nonautonomous system. Phase portraits, power spectra, Poincaré maps, and Lyapunov exponents are presented to observe periodic, quasi-periodic and chaotic motions.

1. Introduction

During the past one and half decades, a large number of studies have shown that chaotic phenomena are observed in many physical systems that possess non-linearity [1,2]. It was also reported that the chaotic motion occurred in many nonlinear control systems [3,4].

The centrifugal governor is a device that automatically controls the speed of an engine and prevents load torque due to sudden change from damaging the engine. It plays an important role in many rotational machines such as diesel engines, steam engines and so on. A simplified version of Vyshnegradskii's analysis of the steam engine with Watt's centrifugal governor is presented by Pontryagin [5], and the stability of the system is also investigated by Hassard et al. [6]. When an engine system is subjected to external disturbances, the speed of the engine

* Corresponding author. Tel.: 00-886-35-712121; fax: 00-886-35-720634.

0020-7225/99/$ - see front matter
PII: S0020-7225(98)00092-5

varies. In order to diminish the change of engine speed, and to avoid the chaotic motion emerging in the operational process of the engine, the regular and chaotic dynamics of a rotational machine with a centrifugal governor are studied in this paper. The mechanical system is assumed to have two different forms of external disturbance. Here, the disturbance can be considered either an initial disturbance (the autonomous case) or a periodic external load (the nonautonomous case).

In Section 2, the governing equations of motion will be formulated, then the stability of the fixed points of the autonomous system are studied by the Lyapunov direct method. In nonlinear dynamical systems, variation of system parameters may cause sudden change in the qualitative behavior of their state. The sudden change of state is referred to as a bifurcation and the parameter value at which the bifurcation occurs is called the bifurcation point. A codimension one bifurcation analysis for the autonomous system is carried out near the degenerate point. The forms of bifurcation will be determined through the process of the local bifurcation analysis. Both the Lyapunov exponents and the Lyapunov dimension will be used to detect the chaos existing in the system.

In Section 3, the nature of the periodic, quasi-periodic and chaotic motions is shown in the phase diagrams, Poincaré maps and power spectra. In order to determine the stability of periodic solutions, various perturbation techniques are employed in weak nonlinear analysis such as the method of averaging [7], and the method of multiple scales [8]. The harmonic balance (HB) [9,10] can be used to treat strong nonlinear systems well but its drawbacks are that a set of complex nonlinear algebraic equations are formulated and must be solved. For higher accuracy, higher harmonic terms are needed and the whole formulation must be

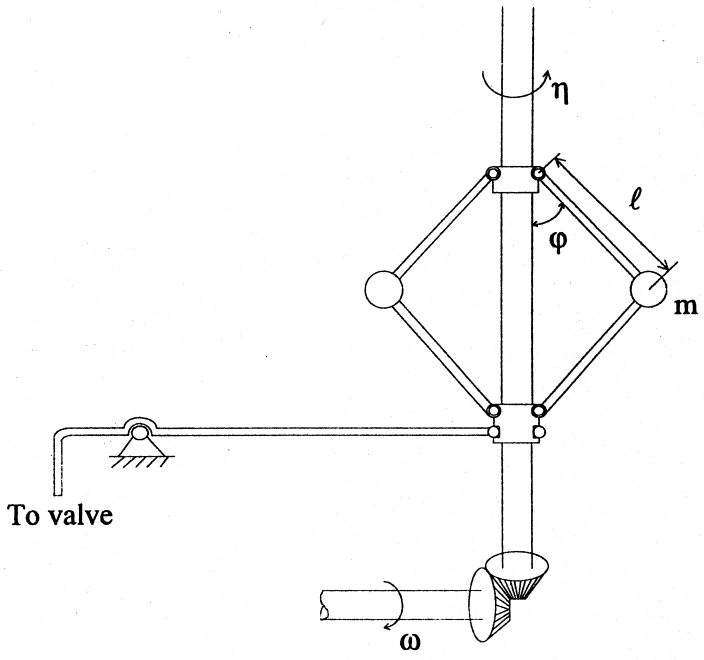

Fig. 1. Physical model of a rotational machine with a fly-ball governor system.

reformed. In comparison, the incremental harmonic balance (IHB) method proposed by Lau et al. [11] which can give accurate results with a few harmonic terms and the accuracy of the results can be increased without difficulty.

In this paper, the IHB method is applied to obtain the periodic solutions of the system. To be more effective, a cubic extrapolation technique [12] is used to predict the neighbouring state from some known states. Thus, the number of iterations required to converge can be further reduced. In addition, the multi-variable Floquet theory [13] is applied to analyze the stability of the periodic solutions.

2. Regular and chaotic dynamics of autonomous systems

2.1. An analytical model

The rotational machine with centrifugal governor is shown in Fig. 1. Some basic assumptions for the system are

1. the mass of the sleeve and the rods is neglected;
2. viscous damping in the rod bearing of the fly-ball is presented by damping constant β.

From Fig. 1, the kinetic and potential energies of the system are written as follows:

$$T = 2 \times \left[\frac{1}{2}m(l^2\eta^2 \sin^2\varphi + l^2\dot{\varphi}^2)\right] = ml^2\eta^2 \sin^2\varphi + ml^2\dot{\varphi}^2,$$

$$V = -2mgl\cos\varphi$$

where l, m, φ and η represent the length of the rod, the mass of the fly-ball, the angle between the rotational axis and the rod, and the angular velocity of the governor, respectively. It is easy to obtain the Lagrangian

$$L = T - V = ml^2\eta^2 \sin^2\varphi + ml^2\dot{\varphi}^2 + 2mgl\cos\varphi.$$

Using the Lagrange equation, the equation of motion is derived

$$\ddot{\varphi} + \frac{\beta}{m}\dot{\varphi} + \frac{g}{l}\sin\varphi = \eta^2 \sin\varphi\cos\varphi. \tag{1}$$

The net torque is the difference between the torque Q produced by the engine and the load torque Q_L, which is available for angular acceleration. That is,

$$J\frac{d\omega}{dt} = Q - Q_L \tag{2}$$

where J is the moment of inertia of the machine. As the angle φ varies, the position of the control valve which admits the fuel is also varied. Their relation is presented by Refs. [5,6], so Eq. (2) is written in the form

$$J\dot{\omega} = \gamma \cos\varphi - P \tag{3}$$

where $\gamma > 0$ is a proportionality constant and P is an equivalent torque of the load.

Usually, the governor is geared directly to the output shaft such that its speed of rotation is proportional to the engine speed, i.e. $\eta = n\omega$. Changing time scale $\tau = \Omega_n t$, Eqs. (1) and (3) can be written in nondimensional form

$$\ddot{\varphi} + C\dot{\varphi} + \sin\varphi = r\omega^2 \sin\varphi \cos\varphi$$

$$\dot{\omega} = k\cos\varphi - F \tag{4}$$

where

$$k = \frac{\gamma}{J\Omega_n}, \quad F = \frac{P}{J\Omega_n}, \quad r = \frac{n^2 l}{g},$$

$$C = \frac{\beta}{m\Omega_n}, \quad \Omega_n = \sqrt{\frac{g}{l}}$$

and the overdot denotes differentiation with respect to τ. Eq. (4) can be expressed as three first order equations

$$\dot{\varphi} = \psi,$$

$$\dot{\psi} = r\omega^2 \sin\varphi \cos\varphi - \sin\varphi - C\psi,$$

$$\dot{\omega} = k\cos\varphi - F, \tag{5}$$

where φ is the angular velocity of the rod. Hence, the dynamics of the system of a rotationing machine with a fly-ball governor is described by a three-dimensional autonomous system.

2.2. Stability analysis by the Lyapunov direct method

Find the equilibria of the system and determine the stability of them. These equilibria can be found from Eq. (5) as $\mathbf{p} = [\varphi_0, 0, \omega_0]$ with

$$\cos\varphi_0 = \frac{F}{k}, \ \omega_0^2 = \frac{k}{rF}.$$

Add slight disturbances x, y, z to the fixed point $(\arccos F/k, 0, \sqrt{k/rF})$

$$\varphi = \varphi_0 + x, \quad \psi = y, \quad \omega = \omega_0 + z. \tag{6}$$

Substitute Eq. (6) into Eq. (5), and expanding $\sin\varphi$, $\cos\varphi$ as the Taylor series, it becomes

$$\dot{x} = y$$

$$\dot{y} = -ax - Cy + bz + \cdots$$

$$\dot{z} = -dx + \cdots \tag{7}$$

where

$$a = \frac{k^2 - F^2}{kF},\ b = \frac{2\sqrt{rkF}\sqrt{k^2 - F^2}}{k^2},\ d = \sqrt{k^2 - F^2},$$

and the terms higher than one degree have not been written down. Let $k > F > 0$, then $a > 0$, $b > 0$ and $d > 0$.

First, asymptotical stability of the null solution of Eq. (7) can be studied by using the Lyapunov direct method. Construct the quadratic Lyapunov function candidate in the form

$$V(x,y,z) = A_{11}x^2 + A_{22}y^2 + A_{33}z^2 + 2A_{12}xy + 2A_{13}xz - 2yz.$$

The derivative of V with respect to τ along the trajectories of the system is given by

$$\dot{V} = -2(aA_{12} + dA_{13})x^2 + (2A_{12} - 2CA_{22})y^2 - 2bz^2 + (2A_{11} - 2aA_{22} - 2CA_{12} + 2d)xy + (2a + 2bA_{12} - 2dA_{33})xz + (2C + 2A_{13} + 2bA_{22})yz + \cdots.$$

Now, it is necessary to choose A_{11}, A_{22}, A_{33}, A_{12} and A_{13} such that V and $-\dot{V}$ are positive definite [14]. Let

$$A_{11} = \frac{ab + a^2b + bC^2 + b^2Cd + C^3d + bd^2}{aC - bd},$$

$$A_{22} = \frac{b + ab + Cd}{aC - bd},$$

$$A_{33} = \frac{a^2C + b^2C - abd + b^3d + bC^2d}{aCd - bd^2},$$

$$A_{12} = \frac{bC + b^2d + C^2d}{aC - bd},$$

$$A_{13} = \frac{b^2 + ab^2 + aC^2}{bd - aC}.$$

Then

$$\dot{V}(x,y,z) = -b(x^2 + y^2 + z^2) + \cdots$$

is negative definite. By Sylvester's theorem [16], the sufficient condition for V to be positive

definite is found:

$$aC > bd$$

i.e.

$$k > \frac{4rF^3}{C^2}. \tag{8}$$

From the Lyapunov asymptotic stability theorem, we conclude that the origin is asymptotically stable. The stability of the origin when $k = 4rF^3/C^2$ has not been obtained by the Lyapunov direct method. In the next subsection, it will be determined by the center manifold and normal form theory.

Next, the stability of the fixed point (arccos F/k, 0, $-\sqrt{k/rF}$) is studied. The differential equations for disturbances are

$$\dot{x} = y,$$

$$\dot{y} = -ax - Cy - bz + \cdots,$$

$$\dot{z} = -dx + \cdots, \tag{9}$$

where a, b, d are the same as above.

In order to determine the instability of the null solution of Eq. (9), the quadratic Lyapunov function candidate is assumed in the form

$$V(x,y,z) = -(a+d)x^2 - y^2 + \frac{a}{d}z^2 - 2(b+C)xz - 2yz.$$

The derivative of V with respect to τ along the trajectories of the system are given by

$$\dot{V} = 2(bd + Cd)x^2 + 2Cy^2 + 2bz^2 + \cdots$$

which is positive definite. There exists the region $V(x,\ y,\ a) > 0$ in the neighborhood of the origin of Eq. (9). Its boundaries in the x–y plane are

$$y = \frac{-d + \sqrt{ad + d^2}}{d}z \text{ and } y = \frac{-d - \sqrt{ad + d^2}}{d}z,$$

in the x–z plane are

$$x = \frac{-(b+C)d + \sqrt{(b+C)^2d^2 + ad(a+d)}}{d(a+d)}z$$

and

$$x = \frac{-(b+C)d - \sqrt{(b+C)^2 d^2 + ad(a+d)}}{d(a+d)} z.$$

In the x–y plane the boundary is

$$z = 0.$$

So, by the Lyapunov instability theorem, the origin is unstable.

2.3. Applications of the center manifold and normal form theory

In nonlinear dynamical systems, variation of system parameters may cause sudden change in the qualitative behaviour of their state. The state change is referred to as a bifurcation and the parameter value at which the bifurcation occurs is called the bifurcation point. Here we give attention to the Hopf bifurcation which will occur in this system. Eq. (7) is rewritten in matrix form

$$\dot{X} = AX + f(X) + O(4), \quad X \in R^3 \tag{10}$$

where $X = [x, \dot{x}, z]^{\mathrm{T}} = [x, y, z]^{\mathrm{T}}$

$$A = \begin{bmatrix} 0 & 1 & 0 \\ \dfrac{F^2 - k^2}{Fk} & -C & \dfrac{2\sqrt{rFk(k^2 - F^2)}}{k^2} \\ -\sqrt{k^2 - F^2} & 0 & 0 \end{bmatrix},$$

$$f = \begin{bmatrix} 0 \\ f_1(X) \\ f_2(X) \end{bmatrix}$$

where

$$f_1(X) = -\frac{3\sqrt{k^2 - F^2}}{2k} y^2 + \frac{rF\sqrt{k^2 - F^2}}{k^2} z^2 + \frac{2(2F^2 - k^2)\sqrt{rFk}}{Fk^2} xy + \frac{4k^2 - 7F^2}{6Fk} x^3 + \frac{r(2F^2 - k^2)}{k^2} xz^2 + \frac{4F\sqrt{rFk(k^2 - F^2)}}{Fk^2} x^2 z$$

$$f_2(X) = -\frac{F}{2} x^2 + \frac{\sqrt{k^2 - F^2}}{6} x^3.$$

The Jacobian matrix A is evaluated at the fixed point $(\arccos F/k,\ 0,\ \sqrt{k/rF})$. Further, it is necessary to find the value of k for which the eigenvalues of A contain a pure imaginary pair with the remaining eigenvalue having a negative real part. The conditions for a pure imaginary pair can be shown to be

$$k = \frac{4rF^3}{C^2}.$$

Here k is considered as the only parameter to be varied for the occurrence of the Hopf bifurcation. When the values of parameters C, F, r are given as 0.7, 1.942, 0.25, respectively, the parameter k takes the critical value

$$k_c = 14.947$$

which is called the bifurcation point.

At this critical parameter k_c, the origin is nonhyperbolic. The eigenvalues of matrix A fail to determine the stability of the fixed point and it becomes necessary to consider the higher order terms to analyze the three-dimensional nonlinear system. So one employs the following methods to analyze the dynamical system. First, the center manifold theorem [15] will be applied to reduce the dimension of the state spaces at the critical parameter k_c. The following linear transformation matrix is used to transform Eq. (10):

$$T = \begin{bmatrix} 0 & \dfrac{C}{2\sqrt{r}F} & \dfrac{C^3}{\delta} \\ \dfrac{\delta}{4rF^4} & 0 & \dfrac{-C^4}{\delta} \\ 1 & 0 & 1 \end{bmatrix}$$

which is formed by eigenvectors of A at k_c, where $\delta = \sqrt{16r^2F^6 - C^4F^2}$. Let

$$\begin{bmatrix} x \\ y \\ z \end{bmatrix} = T \begin{bmatrix} q_1 \\ q_2 \\ q_3 \end{bmatrix}$$

then Eq. (10) is transformed into Jordan form

$$\begin{bmatrix} \dot{q}_1 \\ \dot{q}_2 \\ \dot{q}_3 \end{bmatrix} = \begin{bmatrix} 0 & \dfrac{-\delta}{2C\sqrt{r}F^2} & 0 \\ \dfrac{\delta}{2C\sqrt{r}F^2} & 0 & 0 \\ 0 & 0 & -C \end{bmatrix} \begin{bmatrix} q_1 \\ q_2 \\ q_2 \end{bmatrix} + T^{-1} f(Tq).$$

According to the center manifold theory, it is found that there exists a center manifold tangent to the two dimensional center eigenspace which is formed by eigenvectors corresponding to the pair of pure imaginary eigenvalues. The behavior of the original system in close proximity to the degenerate point can be determined by a two dimensional system restricted within the center manifold $h(q_1, q_2)$.

$$\begin{bmatrix} \dot{q}_1 \\ \dot{q}_2 \end{bmatrix} = \begin{bmatrix} 0 & -2.751 \\ 2.751 & 0 \end{bmatrix} \begin{bmatrix} q_1 \\ q_2 \end{bmatrix} + \begin{bmatrix} 0.059q_1^2 - 0.915q_1q_2 - 0.096q_2^2 \\ 0.015q_1^2 - 0.233q_1q_2 - 0.016q_2^2 \end{bmatrix} +$$

$$\begin{bmatrix} 0.009q_1^3 - 0.005q_1^2q_2 - 0.054q_1q_2^2 - 0.023q_2^3 \\ 0.002q_1^3 - 0.002q_1^2q_2 - 0.014q_1q_2^2 - 0.01q_2^3 \end{bmatrix}, \tag{11}$$

where

$$h(q_1,q_2) = -0.081q_1^2 - 0.001q_1q_2 + 0.086q_2^2 + 0.009q_1^3 - 0.002q_1^2q_2.$$

Next, normal form theory [17–19] is used to study the qualitative properties of the flow restricted on $h(a_1,q_2)$. The method is a local analysis and a sequence of transformation matrices are generated in the neighborhood of the fixed point. The procedure will enable us to simplify the nonlinear terms of Eq. (11) and does not change the qualitative behavior of the system. So Eq. (11) will be written as

$$\dot{y}_1 = 2.751y_2 + (-0.0055y_1 - 0.0086y_2)(y_1^2 + y_2^2) + O(5),$$

$$\dot{y}_2 = 2.751y_1 + (0.0086y_1 - 0.0055y_2)(y_1^2 + y_2^2) + O(5),$$

which is the simplest form of the original system.

One also considers what might occur in the neighborhood of the bifurcation point $k_c = 14.947$. By applying the method used in Ref. [19], we get the unfolding normal form at $k = k_c + \mu$:

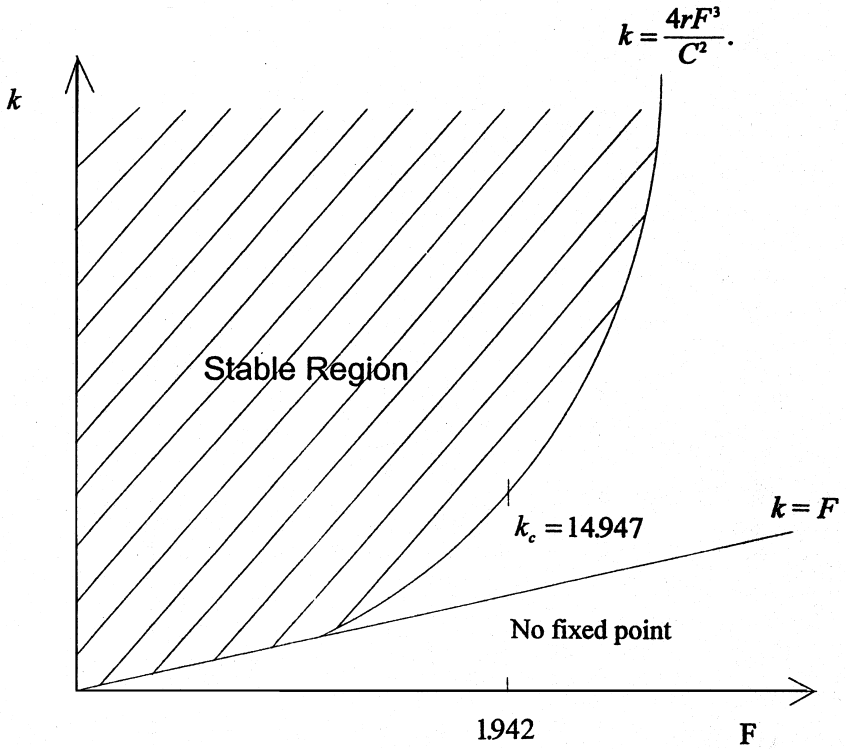

Fig. 2. The stable region of the system.

$$\dot{y}_1 = \mu_1 y_1 - \mu_2 y_2 - 2.751 y_2 + (-0.0055 y_1 - 0.0086 y_2)(y_1^2 + y_2^2) + O(5),$$

$$\dot{y}_2 = 2.751 y_1 + \mu_2 y_1 + \mu_1 y_2 + (0.0086 y_1 - 0.0055 y_2)(y_1^2 + y_2^2) + O(5), \tag{12}$$

where $\mu_1 = -0.011\mu$, $\mu_2 = 0.092\mu$. Change the form of Eq. (12) into polar coordinates and let $y_1 = r\cos\theta$, $y_2 = r\sin\theta$, then

$$\dot{r} = -0.011\mu r - 0.0055 r^3 + O(r^5),$$

$$\dot{\theta} = 2.751 + 0.092\mu + 0.0086 r^2 + O(r^4). \tag{13}$$

The following conditions can be derived from Eq. (13): (1) for $\mu > 0$ ($k > k_c$), the origin is stable; (2) $\mu < 0$ ($k < k_c$), the origin is unstable and forms a limit cycle. It is recognized that the form of the Hopf bifurcation is a supercritical Hopf bifurcation from conditions (1), (2). The stable region of the fixed point (arccos F/k, 0, $\sqrt{k/rF}$) of Eq. (10) is shown in Fig. 2. From the above facts, the center manifold method and normal form method are very useful for analyzing the nonlinear system.

2.4. Lyapunov exponents and Poincaré map

In order to determine the chaos existing in a nonlinear system, the method of detecting the chaos becomes very important. Here a Lyapunov exponent is used as a quantitative measure of the chaotic motion of the system. The Lyapunov exponent may be used to measure the sensitive dependence upon the initial conditions [1]. It is an index for chaotic behavior. Different solutions of the dynamical system, such as fixed points, periodic motions, quasiperiodic motion, and chaotic motion can be distinguished by it. If two chaotic trajectories start close to one another in phase space, they will move exponentially away from each other for a small time on average. Thus, if d_0 is a measure of the initial distance between the two starting points, the distance is $d(t) = d_0 2^{\lambda t}$. The symbol λ is called the Lyapunov exponent. The divergence of chaotic orbits can only be locally exponential, because if the system is bounded, $d(t)$ cannot grow to infinity. A measure of this divergence of orbits is that the exponential growth at many points along a trajectory has to be averaged. When $d(t)$ is too large, a new "nearby" trajectory $d_0(t)$ is defined. The Lyapunov exponent can be expressed as:

$$\lambda = \frac{1}{t_N - t_0} \sum_{k=1}^{N} \log_2 \frac{d(t_k)}{d_0(t_{k-1})}. \tag{14}$$

The signs of Lyapunov exponents provide a qualitative picture of the system dynamics. Positive values of Lyapunov exponents indicate chaos, negative values of Lyapunov exponents indicate a stable orbit. In three-dimensional space, the Lyapunov exponent spectra for a strange attractor, a two-torus, a limit cycle and a fixed point are described by (+,0,−), (0,0,−), (0,−,−) and (−,−,−), respectively [20].

In order to explore the chaos of the fly-ball governor system, three Lyapunov exponents are calculated when the values of parameters C, F, r are given as 0.7, 1.942, 0.25 and k is varied

from 1.942 to 20. Fig. 3 illustrates the fact that some values of parameter k will cause chaotic motion. When one defines $\varphi = x$, $\dot{\varphi} = y$, $\omega = z$, and uses the initial conditions $x(0) = 0.02$, $y(0) = 0.01$, and $z(0) = 0.03$ at: (1) $k = 16$, and (2) $k = 2.603$, three Lyapunov exponents are obtained, respectively,

$$\lambda_1 = -0.008,\ \lambda_2 = -0.0127,\ \lambda_3 = -0.6792,$$

the motion of which converges to fixed point and

$$\lambda_1 = 0.1116,\ \lambda_2 = 0.0,\ \lambda_3 = -0.8116$$

which means chaotic motion. Three Lyapunov exponents for the occurrence of a Hopf bifurcation at $k_c = 14.947$ are 0.0, 0.0002, −0.6998, respectively.

In a dissipative system, the sum of all the Lyapunov exponents is equivalent to the negative value of the coefficient of damping in the system [21]. Hence, the sum of the three Lyapunov exponents for the two cases (1) and (2) are −0.7.

The Poincaré map for different k is used to determine the form of the bifurcation leading the system into chaos. Usually, the period of the trajectories is not explicitly known for the autonomous system, so the choice of the Poincaré section is different from the nonautonomous

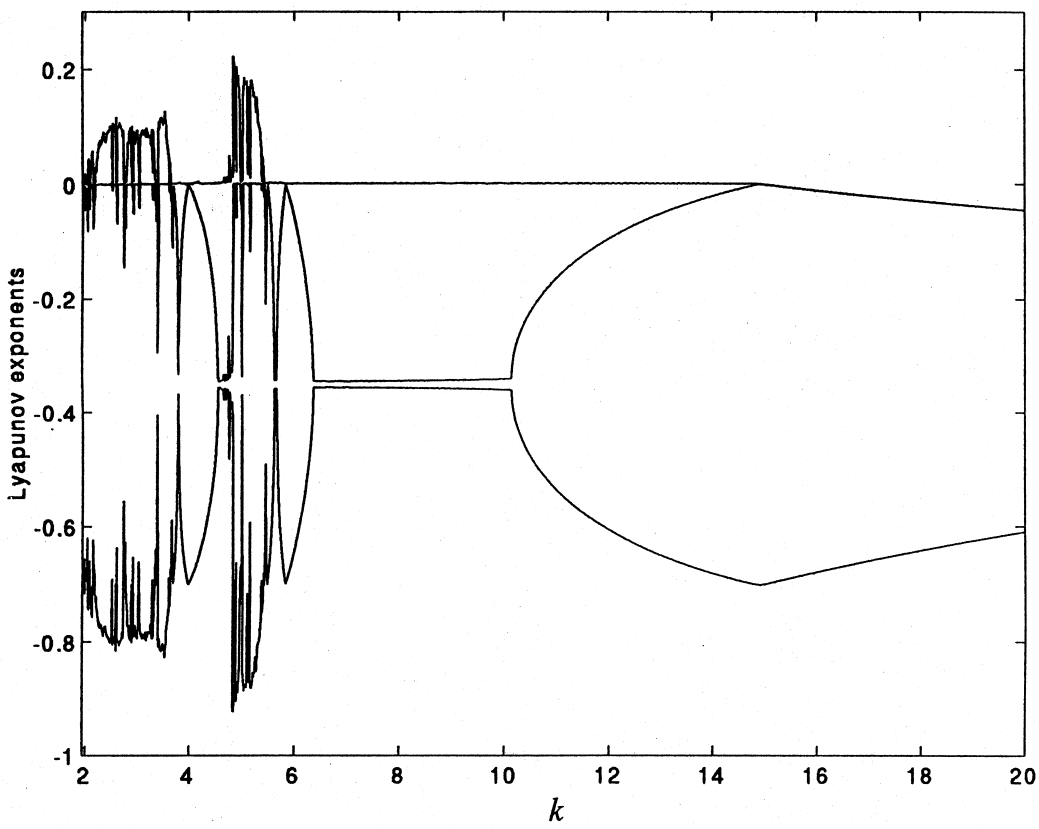

Fig. 3. Three Lyapunov exponents for k between 1.942 and 20.

system. The Poincaré section of the three-dimensional autonomous system Eq. (5) is defined by

$$\Sigma = \{(x,y,z) \in R^1 \times R^1 \times R^1 | z = z_0\}$$

and satisfies the condition

$$\mathbf{n} \cdot (x - x_\Sigma) > 0.$$

The vector $\mathbf{n}$ normal to Σ is given by

$$\mathbf{n} = \begin{bmatrix} 0 \\ 0 \\ 1 \end{bmatrix}$$

and x_Σ is a point located on the section Σ. As k is decreased from the Hopf bifurcation which occurred at $k_c = 14.947$, a cascade of period-doubling bifurcations develops which leads the system into chaos. Fig. 4(a), (b) shows the phase portraits and Poincaré map of the chaotic motion at $k = 2.603$.

In this section, the governing equations of motion of the system are given while the stability

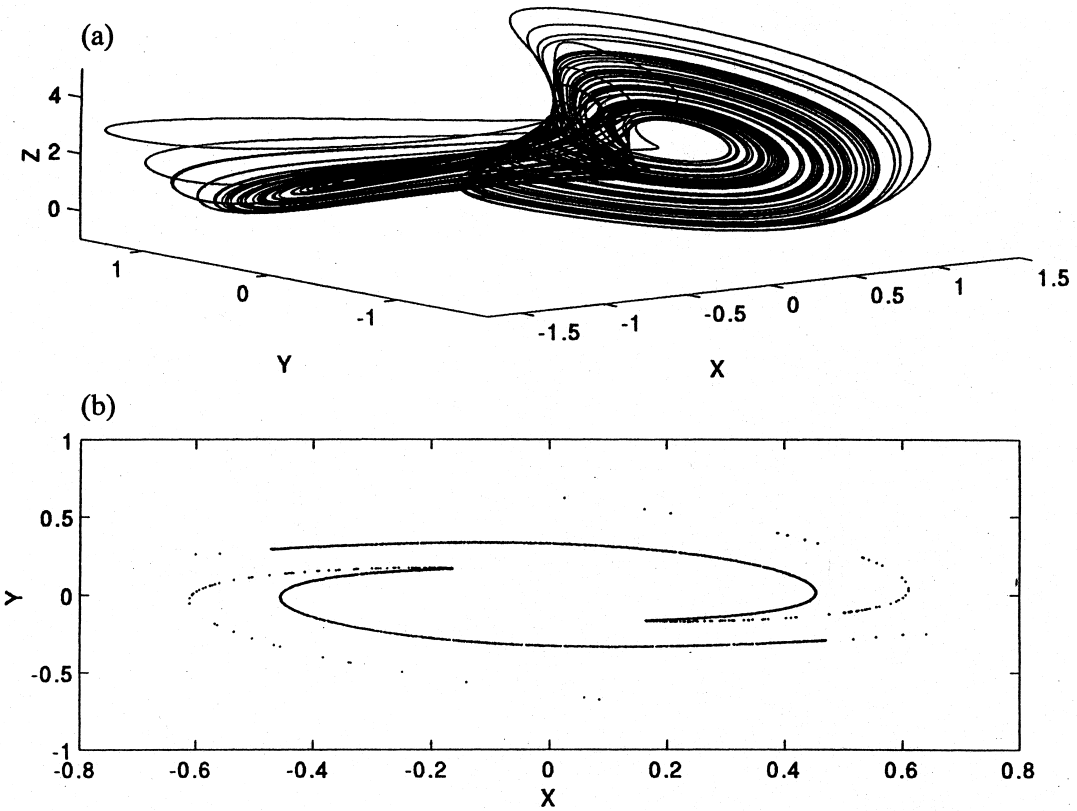

Fig. 4. (a) Phase portrait; and (b) Poincaré map for $k = 2.603$.

of the fixed points are studied by the Lyapunov direct method. Holpf bifurcation analysis is carried out near the degenerate point. A Lyapunov exponent and a Lyapunov dimension are used to show the chaos existing in the system.

3. Regular and chaotic dynamics of nonautonomous systems

In the previous section, the load torque is assumed to be constant for the system. Another condition can be considered. The load torque is now not constant but is represented by a Fourier series consisting of a constant term and a series of harmonic terms. It is reasonable that the load torque of an internal combustion engine repeats after every complete working cycle. For simplicity, the form of the load torque is assumed to be $F + v \sin \bar{\omega} \tau$, where F, v, $\bar{\omega}$ are constants. Denoting $\varphi = x$, $\dot{\varphi} = y$, $\omega = z$, Eq. (4) is rewritten in the form

$$\ddot{x} + C\dot{x} + \sin x = rz^2 \sin x \cos x,$$

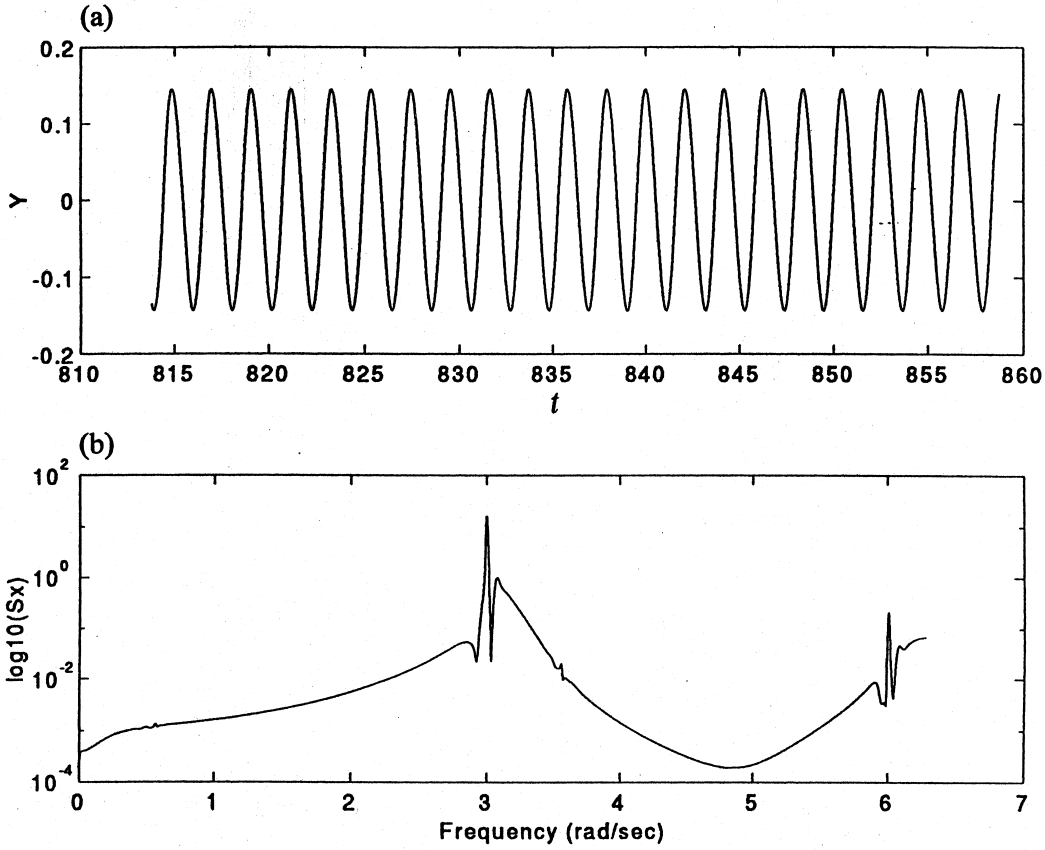

Fig. 5. Show period-1 T motion at $k = 17.8$: (a) time history; (b) power spectrum.

$$\dot{z} = k\cos x - F - \nu \sin \bar{\omega}\tau,$$

where $C = 0.7$, $r = 0.25$, $F = 1.942$ $\bar{\omega} = 3.0$ and $\nu = 0.5$.

3.1. Time history and power spectrum

A valuable technique for the identification and characterization of the system is the power spectrum. It is often used to distinguish between periodic, quasi-periodic and chaotic behaviors of a dynamical system [22,23]. The nonautonomous systems are observed by the portraits of the time history and the power spectrum for $k = 17.8$, 14.5 and 5.13. In Fig. 5(b), the system is in periodic motion, and the power spectrum exhibits a strong peak at the forcing frequency together with super-harmonic frequencies. In Fig. 6(b), the power spectrum of the system consists of two fundamental frequencies ω_1, ω_2, and integer combinations $a_1\omega_1 + a_2\omega_2$ where a_1 and a_2 are small integers [24]. At $k = 5.13$, the chaotic motion appears in Fig. 7(b). The chaotic spectrum is a continuous broad-band one. Although a broad spectrum does not guarantee sensitivity to initial conditions, it is still a reliable indicator of the chaos.

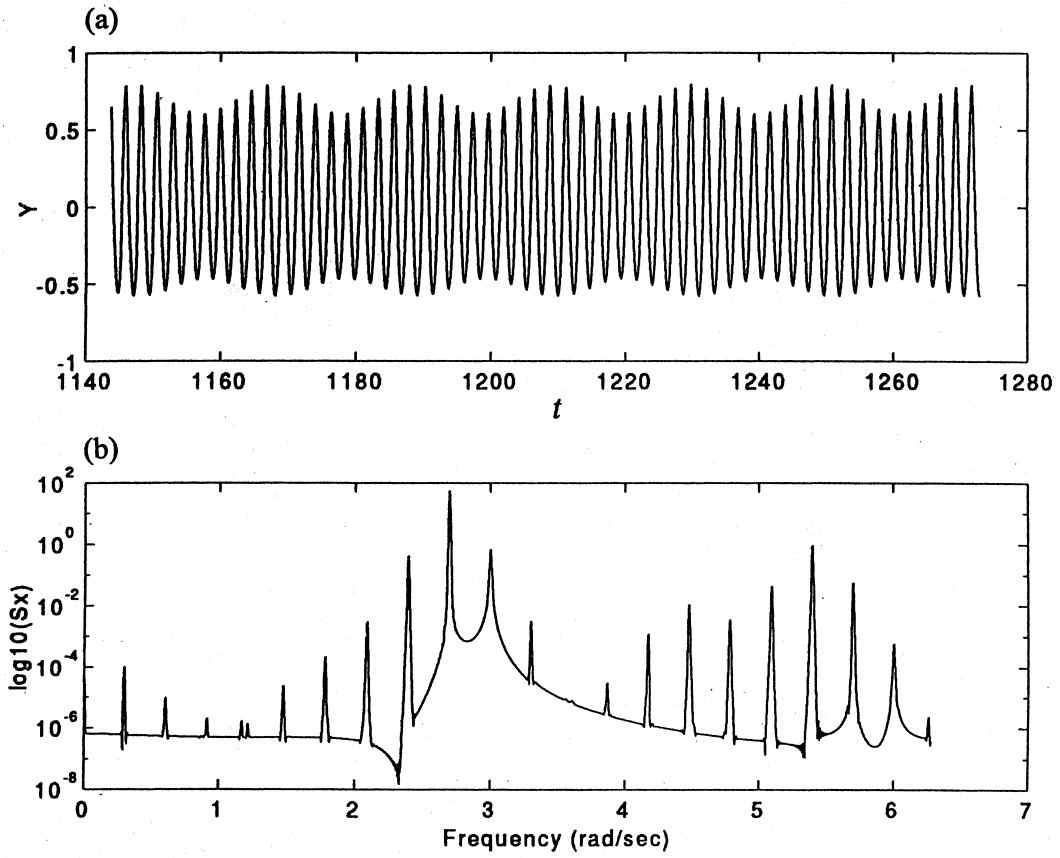

Fig. 6. Show quasi-periodic motion at $k = 14.5$: (a) time history; (b) power spectrum.

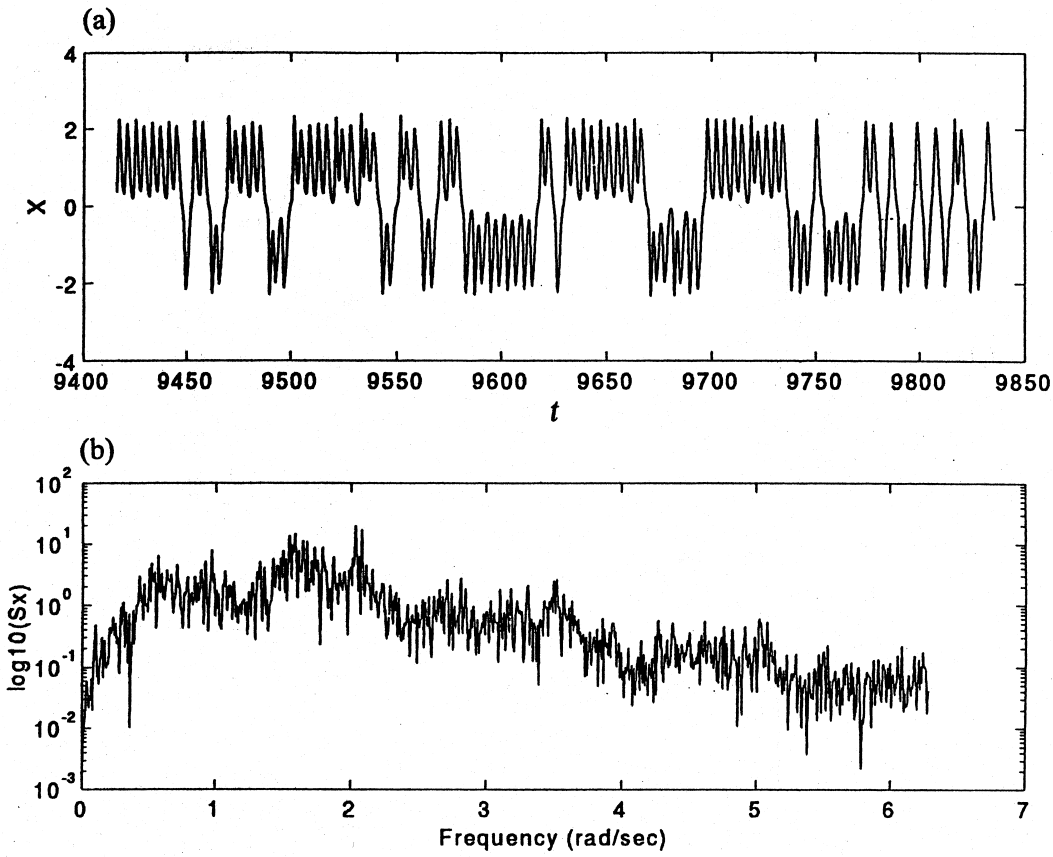

Fig. 7. Show chaotic motion at $k = 5.13$: (a) time history; (b) power spectrum.

Lyapunov exponents are also adopted for distinguishing periodic, quasi-periodic, and chaotic motions. The results shown in Table 1 are also in good agreement with the power spectrum.

Table 1
Lyapunov exponents for different values of k

	Period-T	Quasi-periodic	Chaotic
k	17.8	14.5	5.13
λ_1	−0.027	0	0.172
λ_2	−0.031	−0.015	−0.03
λ_3	−0.642	−0.685	−0.842
λ_4	0	0	0
$\sum_i \lambda_i$	−0.7	−0.7	−0.7

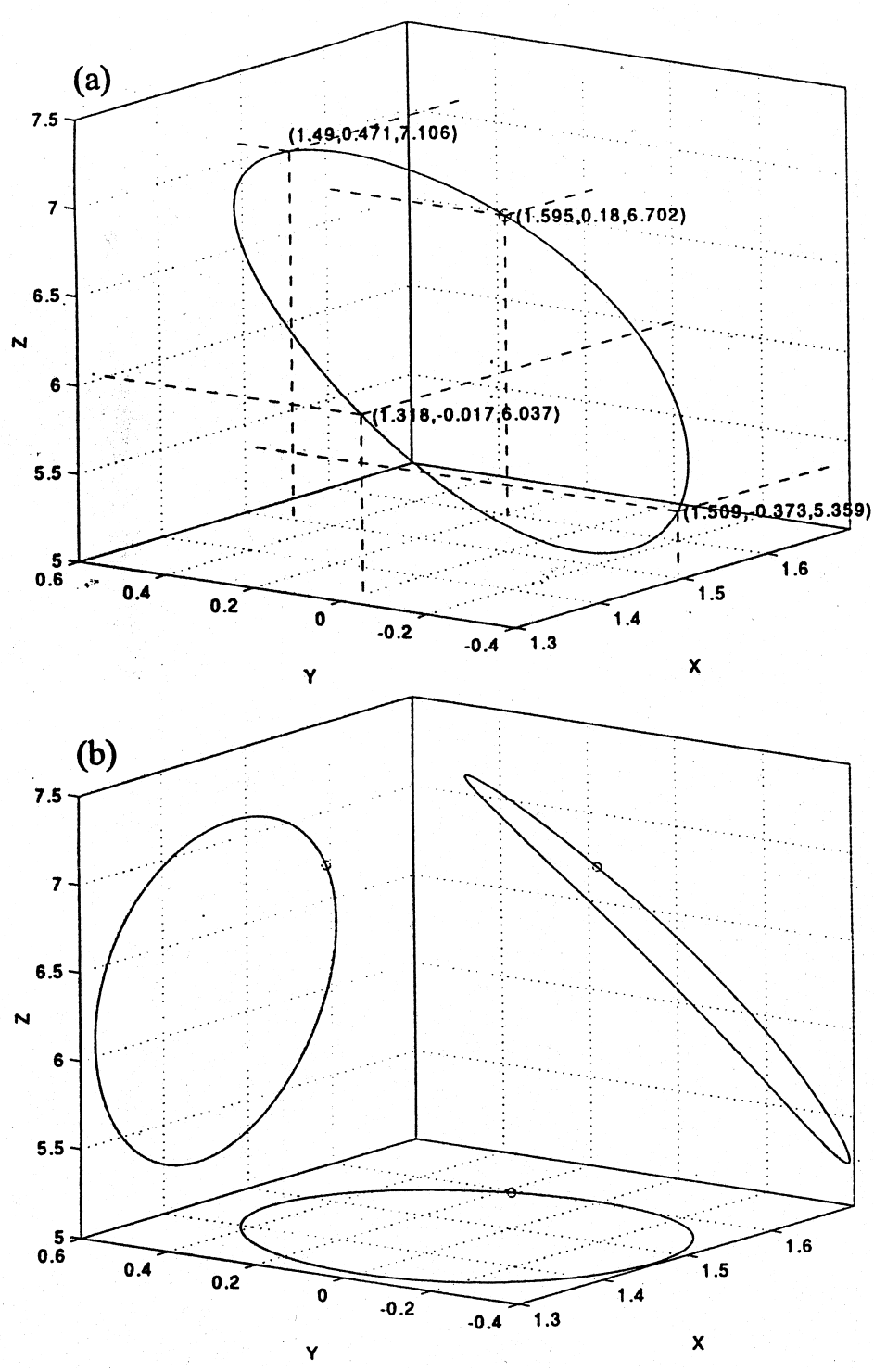

Fig. 8. (a) Phase portrait; and (b) Poincaré map for $k = 17.8$.

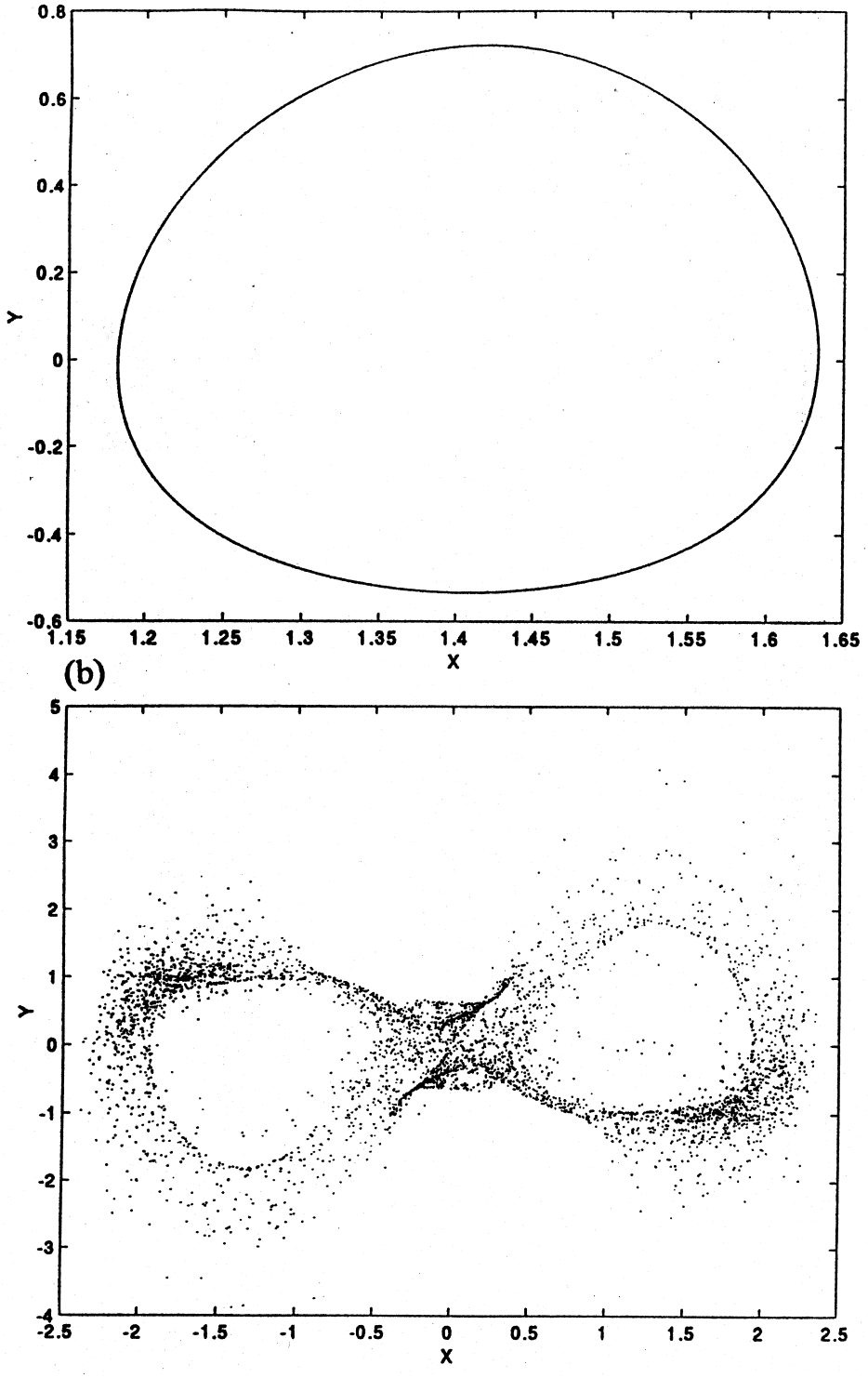

Fig. 9. Projection of Poincaré map of: (a) quasi-periodic; and (b) chaotic motion on x–y plane.

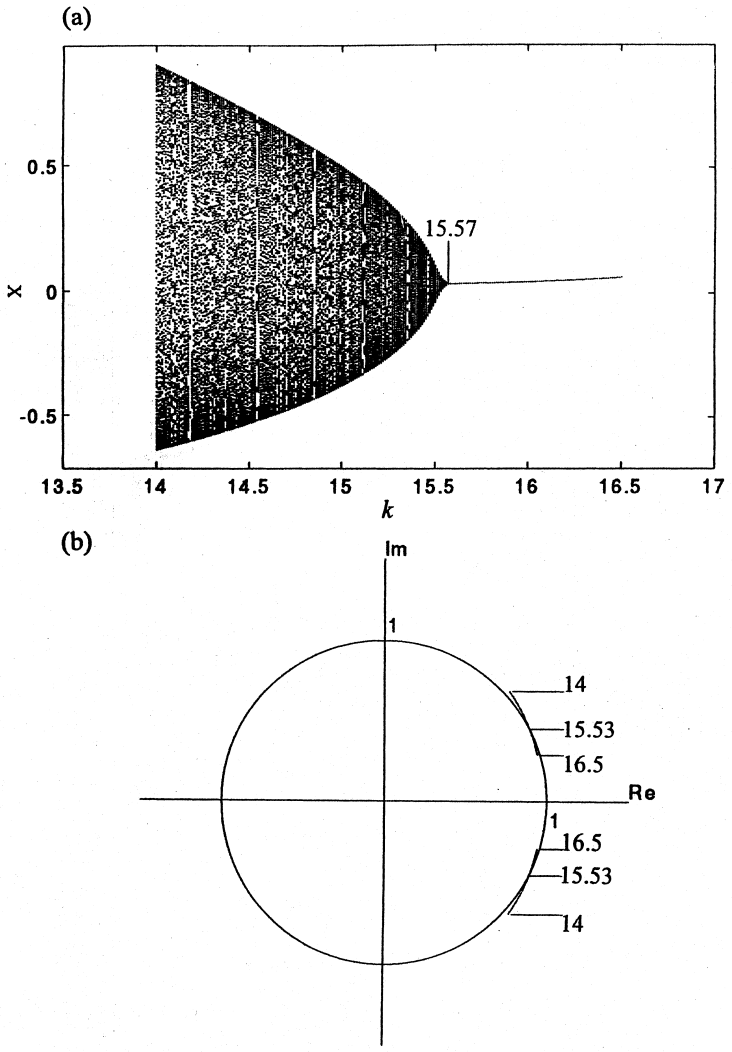

Fig. 10. (a) Bifurcation diagram for k between 16.5 and 14; (b) shows how the Floquet multiplier leave the unit circle for secondary Hopf bifurcation.

3.2. Poincaré map and bifurcation diagram

Now a Poincaré map is adopted to deal with the nonautonomous system where the Poincaré section is prescribed as a $\bar{\omega}\, t = \phi_0 + 2n\pi$ ($\phi_0 = 0$) plane in four-dimensional space (x, $\dot{x}$, z, $\bar{\omega}\, t$). Assuming that the motion of the system starts at an initial time $t = t_0$, the points on the Poincaré section can be collected by a sampling of state variables at intervals of the forcing period $T = 2\pi/\bar{\omega}$. Some numerical simulation results for different k are discussed below. The small circle in Fig. 8(a), (b) for $k = 17.8$ indicates that the system motion is a stable harmonic motion of period $2\pi/\omega$ or period-1 motion. When $k = 14.5$, the system motion is a quasi-periodic motion and the map will form a continuous closed orbit in the Poincaré section as

shown in Fig. 9(a). If the Poincaré map appears as neither a finite set of points nor a closed orbit, the motion may be chaotic. From Fig. 9(b), chaotic motion is seen as $k = 5.13$.

One tries to vary one of the control parameters in the system, and to record the data of the Poincaré map corresponding to every different parameter value. Then, the steady state behavior of the system vs the range of control parameters will be plotted. This is called as a bifurcation diagram. It is a widely used technique to describe a transition from periodic motion to chaotic motion for a dynamical system. The transition sequence of the system studied is from periodic motion to quasi-periodic motion which finally routes to chaotic motion.

From $k = 16.5$ to 14, the bifurcation diagram shown in Fig. 10(a) shows that a periodic solution loses stability at the critical value $k = 15.57$, then a quasi-periodic solution is formed. This is called a secondary Hopf bifurcation. The multi-variable Floquet–Liapunov theory [13] is also applied to observe the change of the qualitative behavior of their state. When k is used as a control parameter and gradually decreased from 16.5, the periodic solution remains stable until the critical value $k = 15.53$ is reached. At this value, a complex conjugate pair of Floquet multipliers crosses the unit circle away from the real axis shown in Fig. 10(b). This bifurcation point and the form of bifurcation are the same as the above result obtained by numerical integration.

3.3. Incremental harmonic balance method

From Eqs. (1) and (3), the natural frequency of the system is given by

$$\omega_{\mathrm{n}} = \sqrt{\frac{(K^2 - P^2)g}{KPl}}.$$

Obviously, ω_{n} depends on the parameters K, P, l and g. Let the dimensionless time be $\tau = \bar{\omega}\, t$ and the frequency ratio be $\Omega = \bar{\omega}/\omega_{\mathrm{n}}$, Eqs. (1) and (3) become

$$\Omega^2\ddot{\varphi} + \xi\Omega\dot{\varphi} + \sigma \sin\varphi = \rho\omega^2 \sin\varphi \cos\varphi,$$

$$\Omega\dot{\omega} = \alpha \cos\varphi - \bar{F} - \varepsilon \sin\tau,$$

where

$$\alpha = \frac{\gamma}{J\omega_{\mathrm{n}}}, \quad \bar{F} = \frac{P}{J\omega_{\mathrm{n}}}, \quad \xi = \frac{\beta}{m\omega_{\mathrm{n}}},$$

$$\sigma = \frac{g}{l\omega_{\mathrm{n}}^2}, \quad \rho = \frac{n^2}{\omega_{\mathrm{n}}^2}$$

and the overdot denotes differentiation with respect to τ.

The procedures of the IHB method for seeking periodic solutions are mainly divided into two steps: (1) the first step is a Newton–Raphson procedure; (2) the second step of the method is Galerkin's procedure. In the computer implementation, the incremental arc-length method

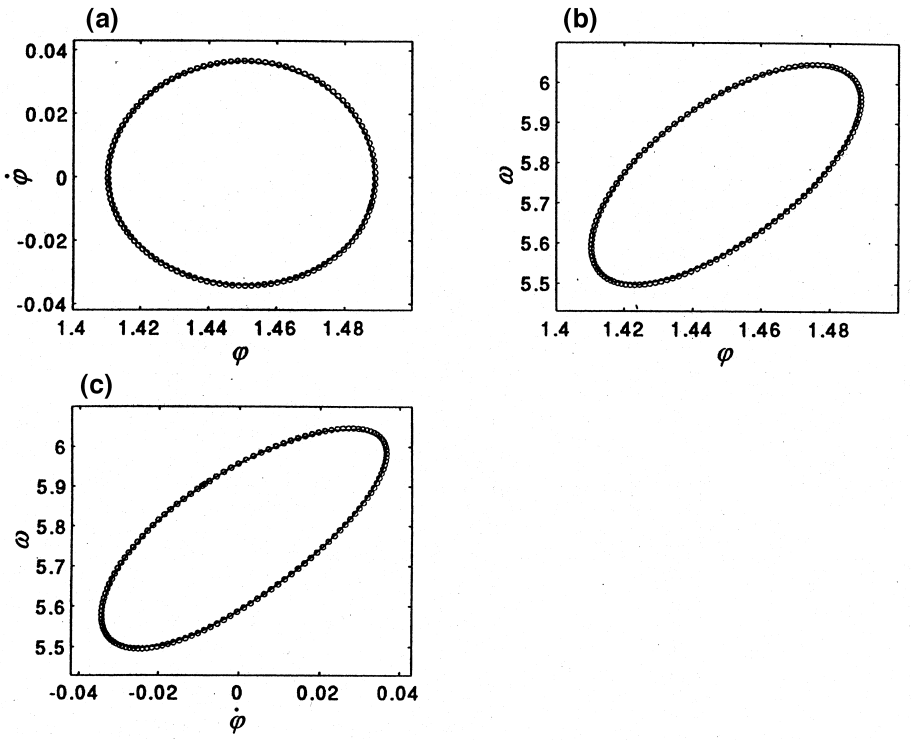

Fig. 11. Comparison between IHB and numerical integration for $\alpha = 5.616$, $\sigma = 0.123$, $\rho = 0.015$, $\xi = 0.24$, $\bar{F} = 0.68$, $\varepsilon = 0.17$. (a) A periodic solution for three state variables φ, $\dot{\varphi}$, ω, projected on φ, $\dot{\varphi}$ plane. (b) the same periodic solution projected on φ, ω plane. (c) The same periodic solution projected on $\dot{\varphi}$, ω plane.

combined with a cubic extrapolation technique [12] are adopted. The technique can predict the next solution from some known states. As such, it will greatly reduce the number of iterations required for the solution to converge. Further, it also overcomes the convergence problem at the sharp peaks of the solution diagram. In our examples $N = 3$ is sufficient to obtain very good and accurate results.

The solutions obtained by the IHB method in comparison with those obtained by numerical integration are shown in Fig. 11, in which the symbols "o" indicate the solution obtained by IHB. These solutions are in good agreement. Figure 12(a) shows the bifurcation diagram obtained by numerical integration and that obtained by the IHB method is plotted in Fig. 12(b). The solid line represents a stable solution and the dashed line represents an unstable solution in Fig. 12(b). Both results are in good agreement with the stable solution as shown in Fig. 13.

4. Conclusions

In this paper, a rotational machine with a centrifugal governor exhibits regular and chaotic behavior when the parameters are varied. In Section 2, the conditions of asymptotic stability

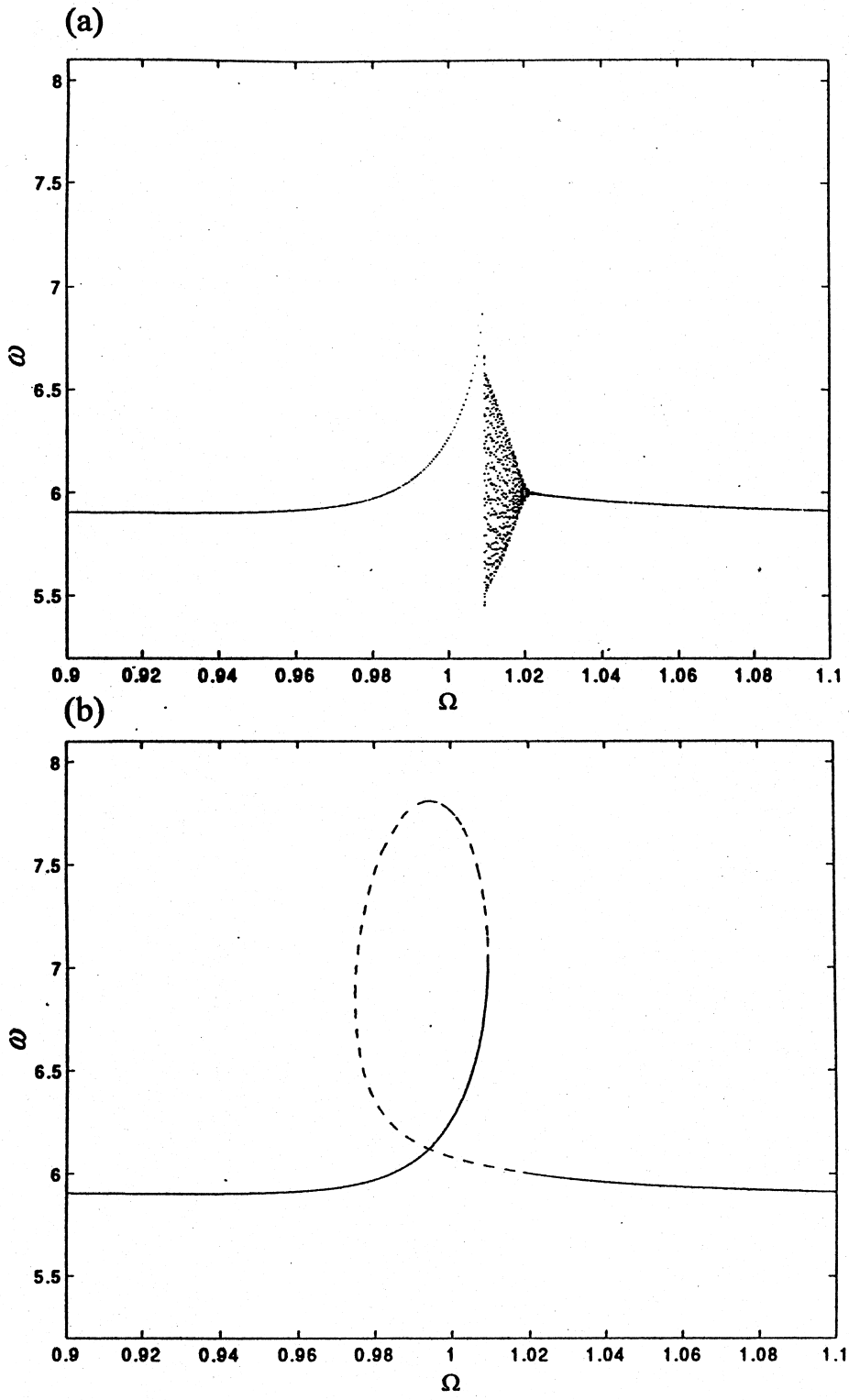

Fig. 12. (a) Shows bifurcation diagram for Ω between 0.9 and 1.1, by numerical integration; (b) shows bifurcation diagram by IHB, —, stable; - - -, unstable.

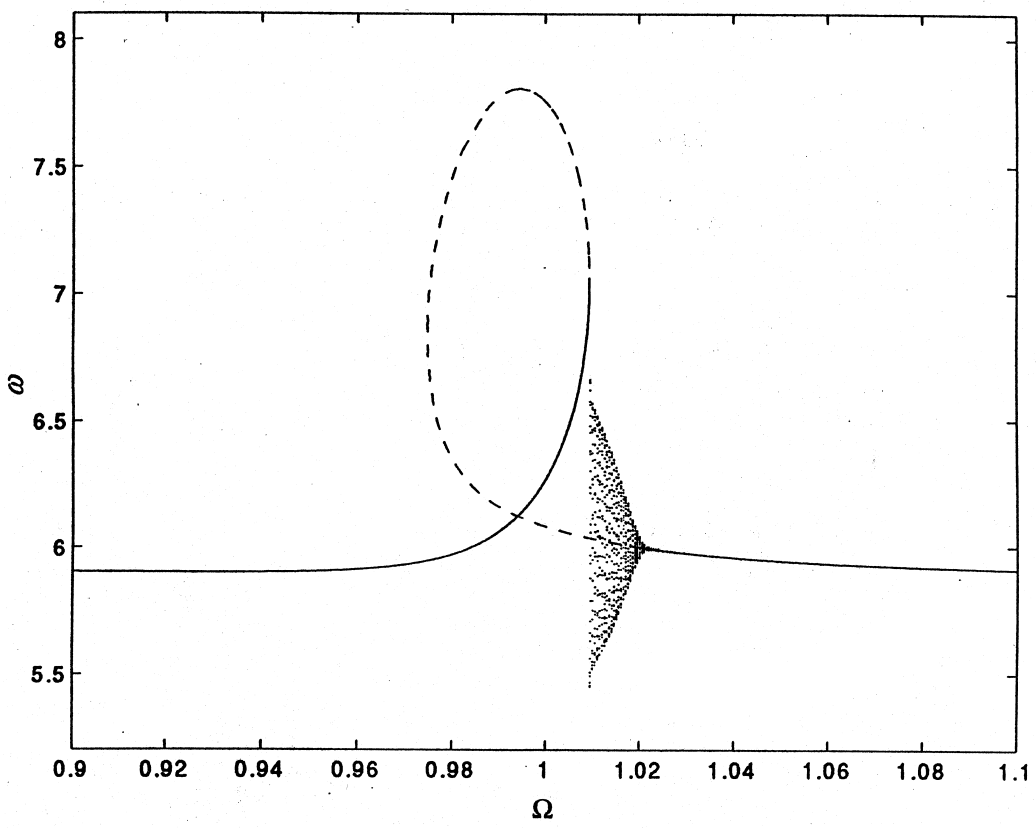

Fig. 13. Comparison between numerical integration and IHB, —, stable; - - -, unstable.

and instability of fixed points have been determined by the Lyapunov direct method. As $k = 4rF^3/C^2$, the equilibrium point (arccos F/k, 0, $\sqrt{k/rF}$) of the system has been shown to be asymptotically stable by the center manifold and normal form theory. The occurrence of a Hopf bifurcation is also found in the autonomous system. By such analysis, these conditions will offer a criterion for the designer on how to decide the parameters of a system for stable situations of engine operation.

For the nonautonomous case, the periodic, quasi-periodic and chaotic motion are obtained by the numerical methods such as power spectrum. Poincaré map and Lyapunov exponents. From the bifurcation diagram, it is also obtained that the system possesses a narrow period-3 window for certain parameters. The steady-state responses of the system are analyzed by the incremental harmonic balance (IHB) method combined with multi-variable Floquet theory, and the numbers of harmonic terms $N = 3$ are sufficient to obtain very good and accurate result. The results obtained by the IHB method are found to match exactly those obtained by numerical integration.

Acknowledgements

This research was supported by the National Science Council, Republic of China, under grant number NSC87-2212-E-009-019.

References

[1] F.C. Moon, Chaotic and fractal dynamics, Wiley, New York, 1992.
[2] J.M.T. Thompson, H.B. Stewart, Nonlinear dynamics and chaos, Wiley, Chichester, 1986.
[3] R.W. Brockett, On conditions leading to chaos in feedback systems, in: Proc. IEEE 21st Conf. Decision and Control, Los Angeles, Wiley, New York, 1982, pp. 932–936.
[4] P. Holmes, Bifurcation and chaos in a simple feedback control system, in: Proc. IEEE 22nd Conf. Decision and Control, Houston, Wiley, New York, 1983, pp. 365–370.
[5] L.S. Pontryagin, Ordinary differential equations, Addison–Wesley, Reading, 1962, pp. 213–220.
[6] B.D. Hassard, N.D. Kazarinoff, Y-H. Wan, Theory and applications of Hopf bifurcation, Cambridge University Press, Cambridge, 1981, pp. 149–156.
[7] J.A. Sanders, F. Verhulst, Averaging methods in nonlinear dynamics, Springer, New York, 1985.
[8] A.H. Nayfeh, Perturbation methods, Wiley, New York, 1973.
[9] P. Sekar, S. Narayanan, Periodic and chaotic motions of a square prism in cross-flow, Journal of Sound and Vibration 170 (1) (1994) 1–24.
[10] O. Gottlieb, Bifurcations and routes to chaos in wave-structure interaction systems, Journal of Guidance Control and Dynamics 15 (4) (1992) 832–839.
[11] S.L. Lau, Y.K. Cheung, Amplitude incremental variational principle for nonlinear vibration of elastic systems, ASME Journal of Applied Mechanics 48 (1981) 959–964.
[12] Y.K. Cheung, S.H. Chen, Application of the incremental harmonic balance method to cubic nonlinear systems, Journal of Sound and Vibration 140 (2) (1990) 273–286.
[13] P. Friedmann, C.E. Hammond, T.H. Woo, Efficient numerical treatment of periodic systems with application to stability problems, International Journal of Numerical Methods in Engineering 11 (1977) 1117–1136.
[14] N.G. Chetayev, The stability of motion, Pergamon Press, New York, 1961.
[15] J. Carr, Applications of Center Manifold Theory, in: Applied Mathematical Sciences, No. 35, Springer, New York, 1981.
[16] J. Guckenheimer, P.J. Holmes, Nonlinear oscillations of dynamical systems and bifurcations of vector fields, Springer, Berlin, 1983.
[17] S. Wiggins, Introduction to applied nonlinear dynamical systems and chaos, Springer, Berlin, 1990.
[18] A.H. Nayfeh, Method of normal forms, Wiley, New York, 1993.
[19] G.X. Li, M.P. Paidoussis, Stability, double degeneracy and chaos in cantilevered pipes conveying fluid, International Journal of Nonlinear Mechanics 29 (1) (1994) 83–107.
[20] A. Wolf, J.B. Swift, H.L. Swinney, J.A. Vastano, Determining Lypunov exponents from a time series, Physica 16D (1985) 285–317.
[21] G.L. Baker, J.P. Gollub, Chaotic dynamics an introduction, Cambridge University Press, Cambridge 1990 Chap. 5.
[22] J.P. Gollub, S.V. Benson, Many routes to turbulent convection, Journal of Fluid Mechanics 100 (1980) 449–470.
[23] M. Ianstiti, Hu Qing, R.M. Westervelt, M. Tinkham, Noise and chaos in a fractal basin boundary regime in a Josephson junction, Physical Review Letter 55 (1985) 746–749.
[24] P.R. Fenstermacher, H.L. Swinney, J.P. Gollub, Dynamical instabilities and the transition to chaotic Taylor vortex flow, Journal of Fluid Mechanics 211 ((1)) (1990) 271–289.